

# Silicon Photomultiplier Choice for the Scintillating Fiber Tracker in Second Generation Proton Computed Tomography Scanner

\*A. Ronzhin<sup>b</sup>, A. Gearhart<sup>a</sup>, E. Johnson<sup>a</sup>, V. Medvedev<sup>a</sup>, V. Rykalin<sup>a</sup>  
P. Rubinov<sup>b</sup>, V. Sleptcov<sup>c</sup>

<sup>a</sup>*Northern Illinois University, DeKalb, IL 60115*

<sup>b</sup>*Fermi National Accelerator Laboratory, Batavia IL 60510*

<sup>c</sup>*Academy of the Development of Device Technology, Moscow Russia*

March 8, 2012

## Abstract

Scintillating fibers are capable of charged particle tracking with high position resolution, as demonstrated by the central fiber tracker of the D0 experiment [1]. The charged particles will deposit less energy in the polystyrene scintillating fibers as opposed to a typical silicon tracker of the same thickness, while SiPM's are highly efficient at detecting photons created by the passage of the charged particle through the fibers. The current prototype of the Proton Computed Tomography (PCT) tracker uses groups of three 0.5 mm green polystyrene based scintillating fibers connected to a single SiPM, while first generation prototype [2] tracker used Silicon strip detectors. The results of R&D for the Scintillating Fiber Tracker (SFT) as part of the PCT detector are outlined, and the premise for the selection of SiPM is discussed.

## Introduction

A Silicon Photomultiplier (SiPM) is a light sensitive sensor originally developed in Russia [3] which consists of a high density matrix of diodes -- pixels with a common output load. Each pixel is operated in a limited Geiger-Miller mode, in order to achieve gain at the level of  $10^6$ . As a consequence, these devices are sensitive to few-photon events even at room temperature and feature a dynamic range defined by the number of pixels. SiPM's may provide excellent time and pulse to pulse resolution [4-6], are insensitive to magnetic fields [7], work well at room temperature, and they are compact and low cost. SiPM's were chosen as the sensors for the fiber tracker subsystem of the PCT prototype.

\*corresponding author

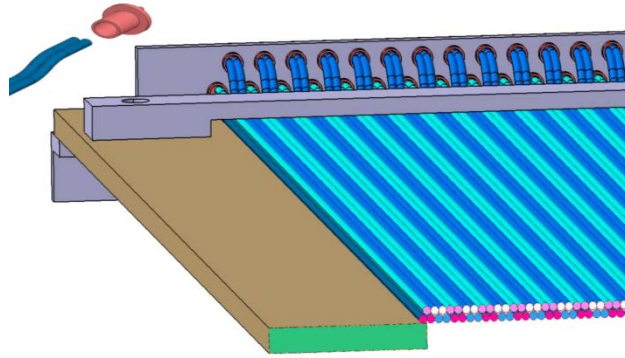


**Fig.1 Possible variant of one plane SFT for pCT tracking detector**

The first generation prototype of the tracking system for the PCT uses a Silicon microstrip detector. It is known that the maximum possible sensitive area for a Silicon microstrip is on the order of 10 cm x 10 cm. The PCT scanner requires a tracking area of 24 cm x 36 cm in order to accommodate a human head, so dead zones had to be introduced into the tracker where Silicon microstrip detectors would slightly overlap with one another, which, in turn, introduces another complication into image reconstruction. The use of scintillating fibers in the tracking system for PCT as shown in Fig. 1 solves the problem of dead zones. According to D0 experience, an area on the order of square meters could be covered without any geometrical inefficiency. But photodetectors used in D0, VLPC counters, arguably the most advanced light sensors currently available, require LHe temperature control along with corresponding equipment, which would increase the complexity of the fiber tracker in many folds. Our choice of SiPMs was based on preliminary Light Yield (LY) measurements when exposing scintillating fibers on 200 MeV proton beam. We used 1 mm diameter Kuraray scintillating fibers directly coupled with one SiPM produced by Center for Perspective Technology and Apparatus, Moscow, Russia, CPTA [8]. The trigger was a 5 cm scintillating fiber placed at the end of a 36 cm fiber in order to account for the attenuation length for the entire length of the fiber. The result of the measurements is shown in Fig. 2. The left distribution is the calibration. The overall result, shown on the right, is ~50 photoelectrons above the noise level of a few Hz at a threshold level of 3 photoelectrons at room temperature. Scintillating fibers of 0.5 mm diameter are expected to have roughly half of the signal of the 1mm scintillating fibers.

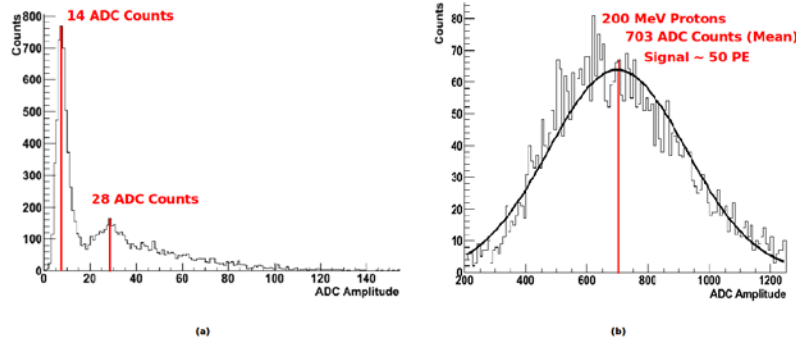


**Fig. 2 LY of 1 mm scintillating fiber coupled to CPTA SiPM for 200 MeV Protons. (a) Calibration of 1 PE, (b) Signal with External Trigger**

Detector characterization is a major task for all applications where SiPM's are used, while, on the other hand, the definition of main parameters is strongly application dependent. For example the Dark Counting Rate (DCR) is an important parameter for evaluation of the noise level and the thermal stability measurement is very important for any application where variation of temperature is expected. Photon Detection Efficiency (PDE) at the wavelength of interest is important for good performance with any application using scintillating fibers. Because the vendor usually supplies the customer with a list of specifications without details of the environment, it was decided to measure a few of the parameters in order to perform a quantitative SiPM analysis of different vendors. After preliminary studies and cost estimation only SiPM's produced by CPTA and IRST/FBK [9] were considered to be used in SFT. Both companies offered SiPM's at a reasonable cost and at a maximum spectral sensitivity in green range. The results of noise measurements, thermal stability, and the number of detected photoelectrons (PE) as an illustration of relative LY were the ground for the choice of the final vendor.

## Hardware

During testing of SiPM's, a Light Emitting Diode (LED) acquired from Industrial Fiber Optics was used rather than a typical radioactive source such as Sr-90. The LED used had a peak wavelength of 530 nm, a spectral bandwidth of 50 nm, and light yield temperature coefficient of  $1.8 \frac{\%}{^{\circ}\text{C}}$  [7]. The scintillating fibers which will be used in the fiber tracker is Kuraray SCSF-3HF(1500)M. The fibers have an emission peak at 530 nm, decay time of 7 ns, and an attenuation length on the scale of 4.5 m [10]. Since the peak spectrum of the LED matched well to the emission peak of the fibers, the LED was connected to the clear fiber, while the other end of the fiber was connected to a SiPM as shown on Fig. 3. The output signal from the clear fiber was measured as roughly 50

photoelectrons, which is significantly lower than the maximum number of pixels from both SiPM vendors.

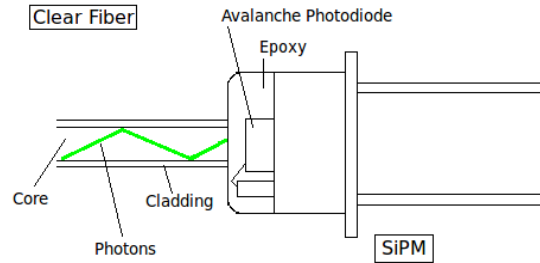


**Fig. 3 SiPM and clear fiber optical connection**

A simple procedure was used for the measurements. A pulse generator was attached to a LED driver and acted as a source to trigger to the Analog to Digital Converter (ADC). The LED driver sent light pulses through the scintillating fiber which was directly coupled to the SiPM. The signal from the SiPM was then sent to the 12 bit ADC for digitization with a rate of 210 mega samples per second. The ADC board, in turn, has a 50 ohm transformer-coupled LEMO input, bias voltage for SiPM, differential amplifier and shaping network.

The ADC output data were then transferred to the PC through the Field Program Gate Array (FPGA) over a USB cable. The ROOT framework was used to analyze the data. A PolyScience chiller [12] was used to maintain temperature inside the housing of the SiPM's with a variation of  $\pm 0.1$  °C. The combined diagram is depicted in Fig. 4. Only the SiPM was placed in a cooled light proof enclosure in order to avoid simultaneous impact of temperature dependence on the LED light yield and on SiPM gain. Ambient and internal enclosure temperatures were recorded during each set of measurements with an accuracy of  $\pm 0.1$  °C. All measurements for the LED light deviations due to temperature variations were normalized according to the vendor's information.

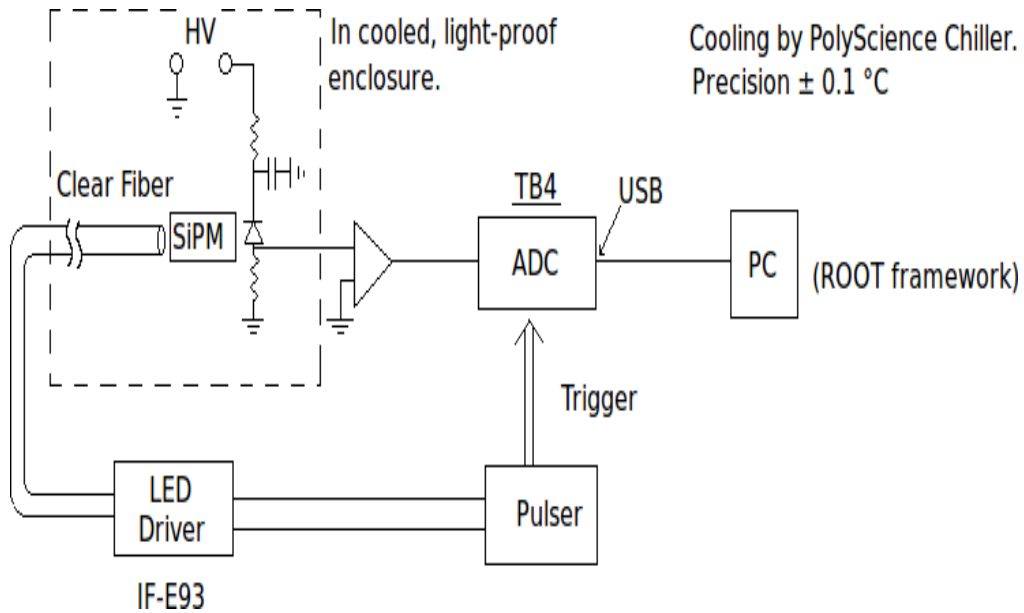


**Fig. 4 Schematic for temperature and relative light yield measurements**

DCR measurements were performed with a slightly different setup. The ADC in was replaced by discriminator with variable threshold as shown in Fig. 5.

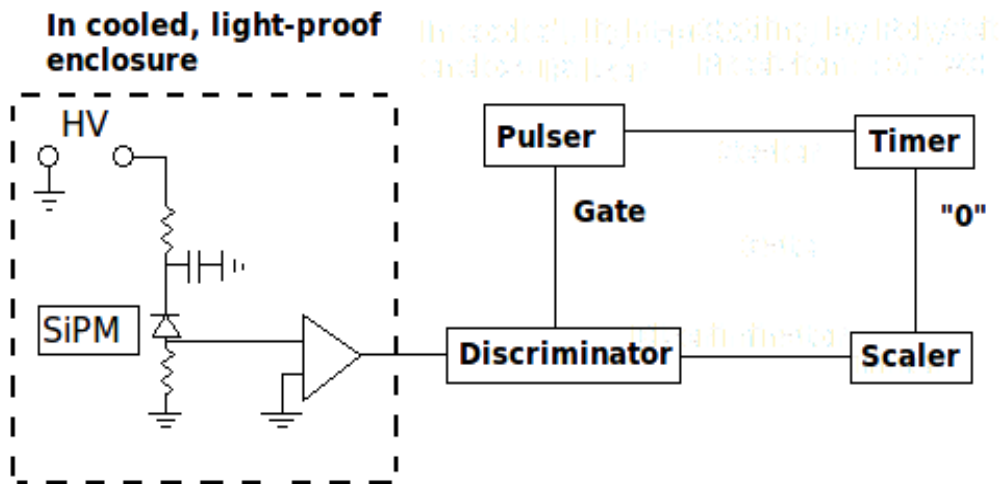


**Fig. 5 Schematic for Noise Calibration**

## Detectors

Manufacturer specifications were compared between the ASD-SiPM1C-M from IRST (labeled with “I” followed by a number) and the CPTA 151 SiPM's (labeled with “R” followed by a number). The CPTA SiPM's have an effective active area of 1.28 mm<sup>2</sup>, while the IRST SiPM's have an effective active area of 1.13 mm<sup>2</sup>. The total number of pixels is 796 and 660 for CPTA and IRST correspondingly. The cell size for CPTA and for IRST is the same ~ 40 x 40 μm<sup>2</sup>. Accordingly the vendors claim the PDE is 18% for the IRST at 480 nm, while the CPTA SiPM's have a PDE around 30% for a wavelength of 600 nm. Because of the absence of details about production technology for particular SiPM batch this information was considered as an input to start comparative measurements rather than setting the base for vendor selection.

## Results

A SiPM is intrinsically a very noisy sensor while working at a threshold of ~ 1 PE. A SiPM pixel can be fired by an incoming photon, but free carries can also be generated by thermal effects or tunneling (field-assisted generation). This effect could lead to frequency of  $\sim 1 \frac{MHz}{mm^2}$  at 25°C with a threshold at  $\frac{1}{2}$  PE amplitude.

The optimum value of threshold depends on signal level and possibility on coincidence scheme. The amplitude for a single PE was determined from the lowest amplitude measured by scope of the most frequent signal. Using this information, noise frequency was plotted against threshold expressed in PE for two different sensors (R4 and 1650-7). The same measurements were repeated for 10 samples from each vendor. No noticeable difference was observed between the two vendors. This was cause to conclude that the noise characteristics of the two vendors are very similar and that one vendor was not preferable for the PCT project. Both sensors could be used without coincidence readout at threshold of 3-4 PE while working at room temperature.

Parameters such as amplification, detection efficiency, and intrinsic noise depend directly on the bias voltage applied. This dependence varies from one SiPM to another, which requires that a unique bias voltage (operating point or OP) needs to be chosen for these parameters. DCR for a particular bias voltage decreases dramatically based on the value of the applied threshold. DCR generally increases with bias voltage increases, however there is a short range of bias voltage where a plateau is seen in the DCR. After a certain value of bias voltage, an increase in voltage does not increase the amplification, but the noise begins to dominate the DCR. In order to find the OP, first the DCR is measured along with a constant light signal. Then only the DCR is measured. The ratio of the DCR plus the signal to the DCR will produce a sharp peak at

a certain voltage. This voltage is defined as the operating OP, and is chosen so that different SiPM's can be compared equally [7].

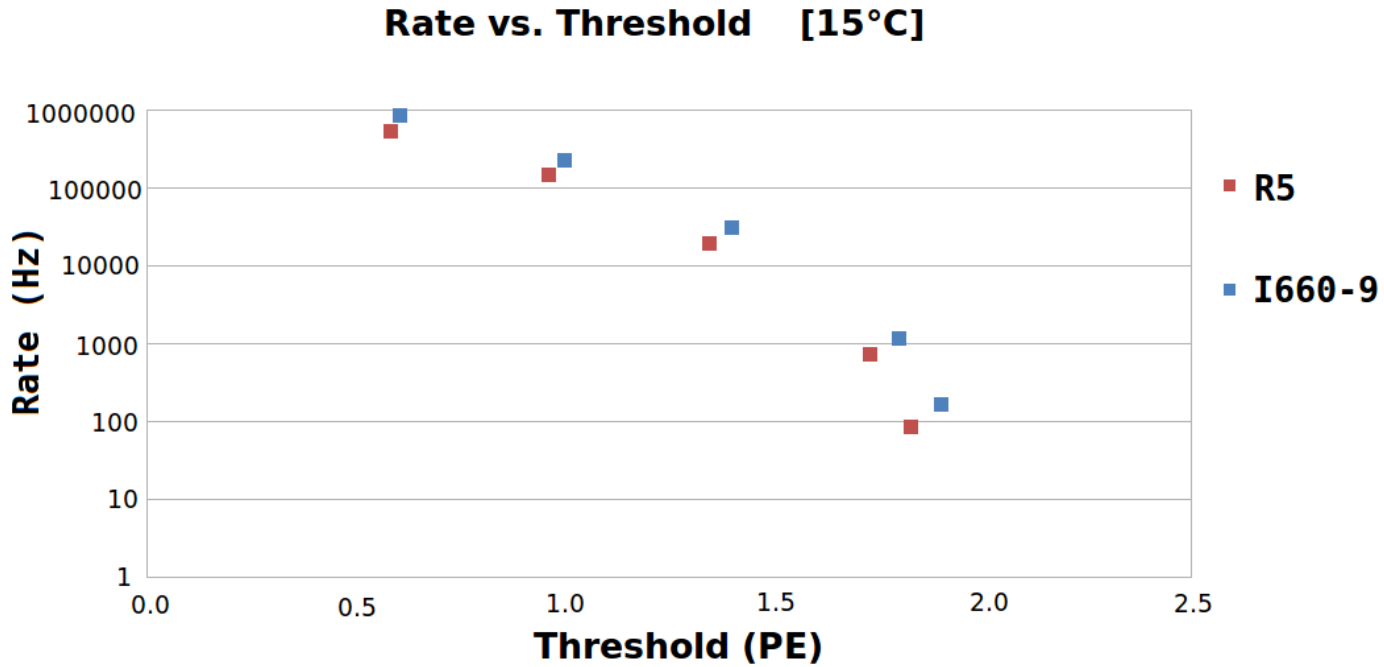
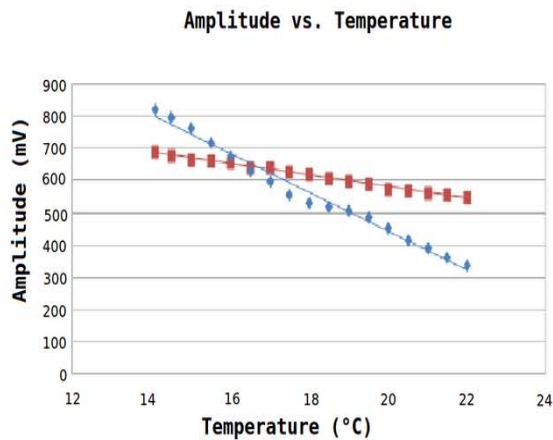
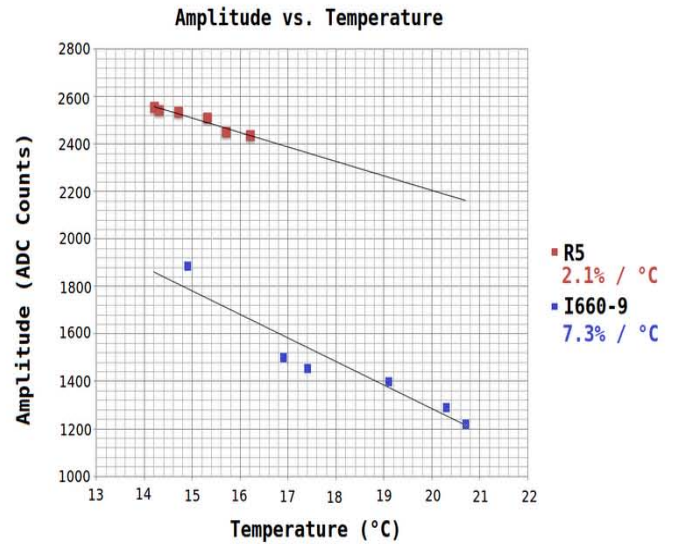


**Fig. 6 Rate vs. Threshold expressed in PE**

Next the amplitude temperature dependence of the various SiPM's was determined. For these measurements, threshold and bias voltage were held constant while the temperature varied. On average the amplitude for the CPTA SiPM's changed  $2.1 \frac{\%}{^{\circ}\text{C}}$ , while for the IRST SiPM's amplitude changed  $7.3 \frac{\%}{^{\circ}\text{C}}$  as shown in Fig. 7.



(a)



(b)

**Fig. 7 Temperature Dependence of CPTA and IRST SiPM's (a) The first set of measurements (no LED temperature compensation), (b) Second set . Normalized for LED Temperature Variation**

The PDE of both CPTA and IRST SiPM's has been compared as a function of wavelength [13]. The emission spectrum of the Kuraray scintillating fibers used in the PCT trackers is shown in Fig. 8 along with the photon detection efficiency of the different SiPM's as a function of wavelength. The emission Spectrum of the fiber was estimated from the manufacturer's specifications for the SCSF-3HF(1500)M fiber [11].

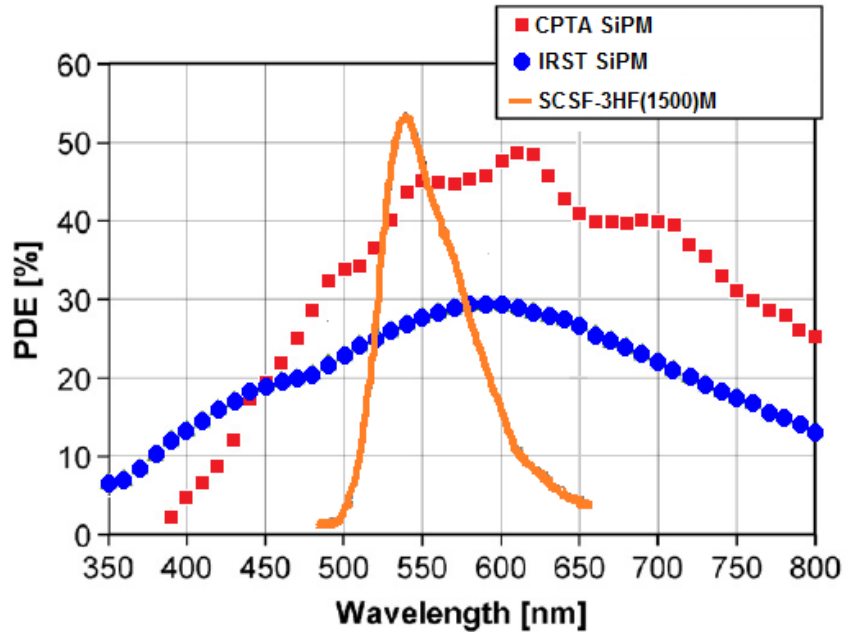


**Fig. 8. PDE vs. Wavelength Overlaid with Estimated Emission Spectrum of Kuraray SCSF-3HF(1500)M Fiber**

Relative light yield measurements were taken in order to confirm or to contradict what was previously measured. The SiPM production technology has many technical aspects that may in turn impact on the final light yield. As the first step for relative LY measurements the pedestal was found and a noise calibration was performed. The pedestal value of around 15 ADC counts was found. The pedestal spread, shown on Fig.9, was measured while the detector was biased before the breakdown point.

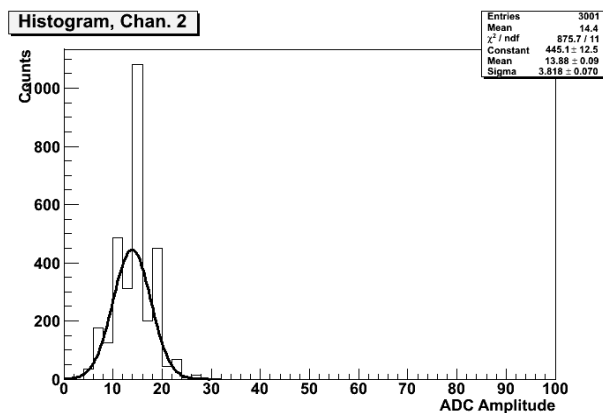


**Fig. 9 Pedestal of ADC**

Gain calibration or the first electron position measurement was performed in order to quantify relative LY. At this time both SiPM's were biased at the operating point at this time whose definition was discussed earlier. The first peak of this distribution accounts for the pedestal of the system SiPM + ADC. The first fitted peak to the right is the position of the first PE, which, simultaneously could be a SiPM gain definition.

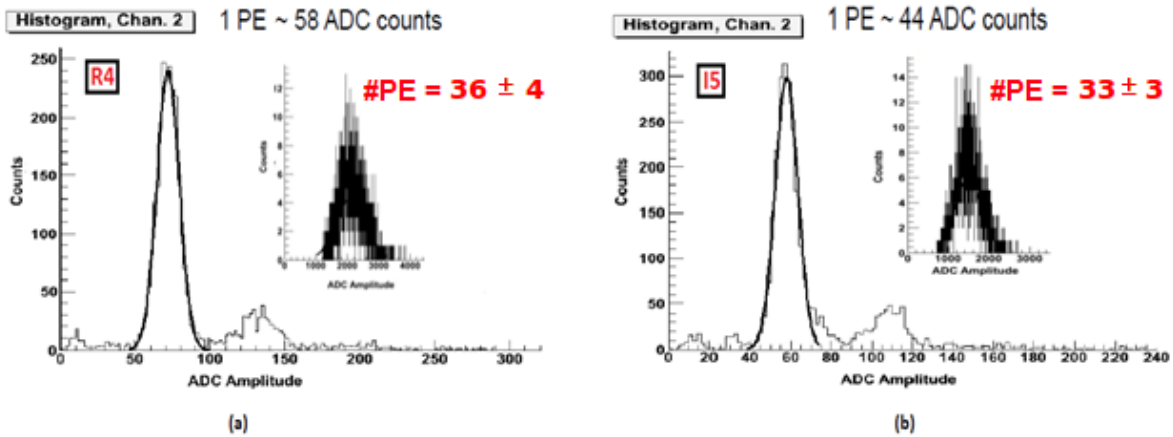


**Fig. 10 Measurements of ADC amplitude of 1 PE inset with the LED signal measurement (a) shows the measurement for the CPTA SiPM, and (b) shows the measurement for the IRST SiPM**

Calibration distributions for the SiPM's of the two different vendors are shown on Fig. 10. While calibrating the position of the first PE no LED signal was used. This is the pure noise calibration that could be applied successfully for a multichannel system. The same procedure of calibration was followed for several sensors of two vendors. After the pedestal was found, the amplitude of 1 PE can be calculated by subtracting the pedestal from the mean of the first peak. Afterwards the same level of signal was applied to the LED Clear Fiber band. The number of PE for the LED signal is determined by dividing the average amplitude measured with the LED by the amplitude of 1 PE. The reproducibility of the signal at the level of 5 % was reached. Signal reproducibility is defined while removing and inserting the clear fiber from an optical interface. The result is depicted in Fig. 11 where the results of LY measurements for 4 SiPM's of the two vendors were averaged.

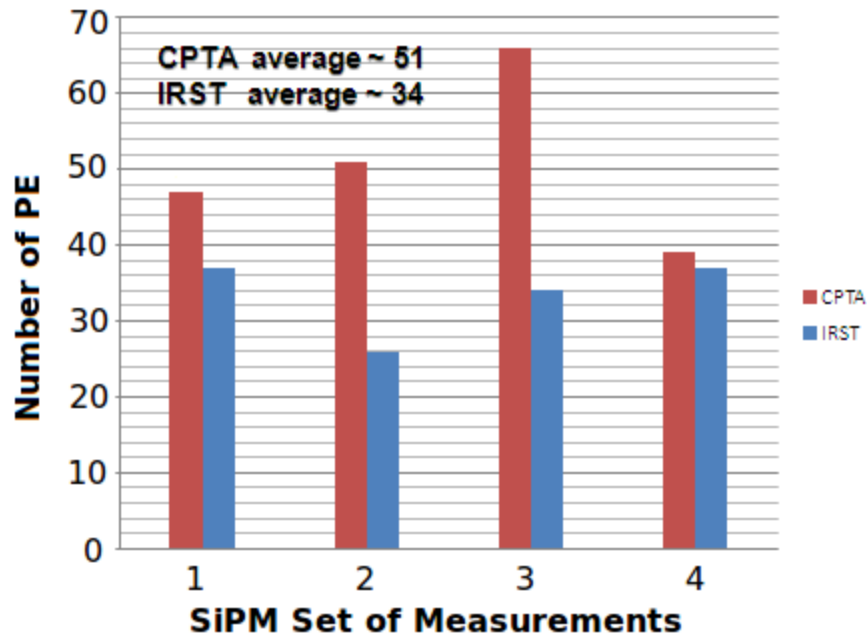


**Fig.11 Measurement of relative LY for the 4 different sensors from CPTA and IRST**

The results of relative LY are shown in Fig. 11 for both SiPM's. One notable fact is that few sensors show similar behavior, which could only be explained by some difference in the technology of the entrance window fabrication, which significantly differs between the two vendors.

The second generation detector for the PCT project demands a data rate around 5 MHz in order to collect imaging data from the patient in a reasonable time frame (~ 10 min.). The most critical role for the tracker will be the internal dynamic characteristics of the SiPM's. Pulse duration depends on the number of pixels fired and the magnitude of the biasing resistor [3]. The recovery time is tunable with the choice of quenching resistor (biasing) with time constant  $\tau \sim R_{\text{bias}} * C_{\text{pixel}}$ , whose value may vary between 20 - 500 ns. For example, with a biasing resistance of 1 M $\Omega$  and a pixel capacitance of 30 fF, the time constant would be 30 ns. These parameters are subject to change since they also impact the after pulsing level as well as other performance characteristics [7]. Direct pulse measurement of particular sensors with a geometrical factor and optimal sensitivity in the green spectrum range were of interest.

The variation of OP was measured for samples of 16 SiPM's from each vendor using the methods described earlier. The values were then averaged over the 16 samples. CPTA SiPM's had an operational point of 43.2 +/- 0.9 V, while IRST SiPM's had an operational point of 43.7 +/- 1.2 V.

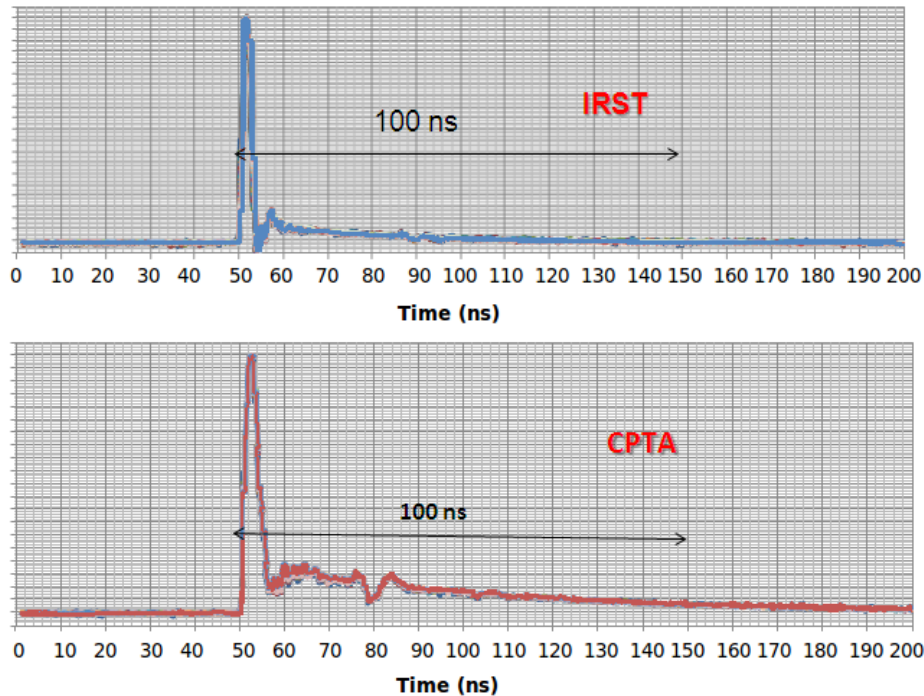


**Fig.12 Direct pulse duration measurement with green laser excitation**

Both CPTA and IRST SiPM's are capable of operating at a 5 MHz rate, as shown in Fig. 12, which shows the relative amplitude plotted against time in ns. While at the same time, with a higher proton rate of the order of 10 MHz, SiPM's produced by IRST have a shorter pulse duration. This set of measurements was taken by direct scope measurement of a Tektronix TDS 3054 with a sampling rate of 5 GS/sec [10], while flashing laser light through a clear optical fiber. The input pulse amplitude was held constant in both measurements in order to avoid excessive pixel firing, which in turn increases pulse duration. The laser pulse width did not exceed 1 ns, which is the limit of accuracy. SiPM's from both vendors have excellent rise time, which would make it possible for their application in many branches of physics; particularly in Positron Emission Tomography [14]. As a result of the evaluation of rate capability, SiPM's from both vendors would perform well for the PCT project. One additional test was performed to illustrate the rate capability of the SiPM's using 200 MeV protons. Scintillator plates of 1 mm thickness wrapped in Tyvek and black paper was directly read out by a fast Photomultiplier (PMT). Another scintillator plate of 3 mm thickness with grooved 1.2 mm Wavelength Shifting Fiber (WLS) was read out by the R4 CPTA SiPM with an operational amplifier. The same TDS 3054 oscilloscope was used to observe the two signals simultaneously with the trigger signal coming from the PMT as shown in Fig. 13. No significant difference between the PMT and SiPM detecting rate capability was observed. However, some after-pulse ringing was due to the SiPM 50  $\Omega$  cable



**Table 1**

Parameter Measured	CPTA	IRST
Avg. # PE of 4 SiPM's Measured	51	34
Temperature Dependence of Amplitude	2.1 $\frac{\%}{^{\circ}\text{C}}$	7.3 $\frac{\%}{^{\circ}\text{C}}$
Rate Limit (current version, direct pulse shape measurements)	> 5 MHz	> 10 MHz
Mean Value of Operation Point and its Spread (STD) over 16 Samples	43.2 V $\pm$ 0.9 V	43.7 V $\pm$ 1.2 V

## References

- [1] D. Adams et. al., "Cosmic ray test results of the D0 prototype scintillating fiber tracker", Nucl. Phys. B Proc. Suppl. 44 (1995) 332-339
- [2] F. Hurley et. al., "Water-Equivalent Path Length Calibration of a Prototype Proton CT Scanner", Med. Phys. 38 (2011) 3568
- [3] V. Golovin , V Savelev, "Novel type of avalanche photodetector with Geiger mode operation", Nucl. Instr. and Meth. A 518 (2004) 560-564
- [4] A. Ronzhin et. al., "Tests of timing properties of silicon photomultipliers", Nucl. Instr. and Meth. A 616 (2010) 38-44
- [5] A. Ronzhin et al., "Development of a 10 ps level time of flight system in the Fermilab Test beam facility", Nucl. Instr. and Meth. A623, 2010, 931-941.
- [6] A. Ronzhin et al., "Waveform digitization for high resolution timing detectors with silicon photomultipliers", Nucl. Instr. and Meth. A668, 2012, 94-97.
- [7] V. Rykalin et. al., "Studies of silicon photodetectors for scintillator-based Hadron Calorimetry at the International Linear Collider", Nucl. Instr. and Meth. A 567 (2006) 62.
- [8] Z. Sadygov et al. Nucl. Instr. and Meth. A, 504 (2003), p. 301
- [9] C. Piemonte et al. IEEE Trans. Nucl. Sci., NS-54 (2007), p. 236
- [10] Industrial Fiber Optics i-fiberoptics.com/pdf/IFE93.pdf
- [11] Kuraray America Inc., 200 Park Ave, NY 10166, USA; 3-1-6, Nihonbashi, Chuo-Ku, Tokyo 103-8254, Japan.
- [12] [http://www.polyscience.com/\\_pdf/\\_manual/\\_recirculating-chillers/110-445.pdf](http://www.polyscience.com/_pdf/_manual/_recirculating-chillers/110-445.pdf)
- [13] Y. Musienko, "Advances in multipixel Geiger-mode avalanche photodiodes" Nucl. Instr. and Meth. A 598 (2009) 213-216
- [14] [http://www.tek.com/sites/tek.com/files/media/media/resources/41W\\_12482\\_19.pdf](http://www.tek.com/sites/tek.com/files/media/media/resources/41W_12482_19.pdf)